Soil Dynamics and Earthquake Engineering 179 (2024) 108502

Contents lists available at ScienceDirect

Soil Dynamics and Earthquake Engineering

journal homepage: www.elsevier.com/locate/soildyn

Generalized Rankine solutions for seismic earth pressures: Validity, limitations & refinements

Panos Kloukinas [a], George Mylonakis [b,c,*]

[a] School of Engineering, University of Greenwich, UK
[b] Department of Civil and Environmental Engineering, Khalifa University, Abu Dhabi, UAE
[c] Department of Civil Engineering, University of Bristol, Bristol, UK

ARTICLE INFO

Keywords:
Seismic Earth pressures
Retaining walls
Limit analysis
Rankine
Lower bound

ABSTRACT

The conditions giving rise to a uniform Rankine stress field involving straight stress characteristics in the soil behind a gravity retaining wall under pseudo-dynamic loading, are revisited. Considering combined gravitational and seismic body forces, exact closed-form solutions are derived for: (1) the coefficients of active and passive earth pressures, (2) the critical values of the five governing problem parameters required to generate the Rankine stress field i.e., wall inclination, wall roughness, backfill inclination, soil friction angle, and body force vector inclination. It is shown that the above parameters are not independent, as the critical value (termed "Rankine value" in this paper) of any of them can be derived as a function of the rest. It is further shown that when the critical wall roughness required to generate a Rankine stress field is smaller, in absolute terms, than the actual wall roughness, the generalized Rankine solution is conservative, overestimating active earth pressures and overestimating the passive, although it does not correspond to a limit state. When this condition is violated i.e., when the critical wall roughness is larger, in absolute terms, than the actual one, the trend reverses and the Rankine solution becomes both unconservative and not physically realizable. Further, if the Rankine wall roughness changes sign (i.e., turns negative for active conditions or positive for passive), the solution becomes even more conservative, yet implicitly corresponds to a kinematically unfeasible wall movement. A parametric investigation of these solutions is provided, with emphasis on practical situations and numerical examples, shedding light into the physics of the problem.

1. Introduction

The origins of modern earth pressure theory can be traced back to the pioneering works of Coulomb (1776) and Rankine (1857) [1,59], who founded two parallel schools of limit analysis, namely the kinematic and the stress approach [2–8]. Ancestor of today's kinematic limit analysis methods is Coulomb's limit equilibrium approach (as extended by subsequent investigators, notably Müller-Breslau [9]) based on the equilibrium of a triangular soil prism formed by two planar yield surfaces, Fig. 1: the soil-wall interface (inclination, ω and roughness, δ_w) and a planar yield surface in the soil mass (inclination unknown and roughness, φ) emerging from the wall base, the inclination of which is optimized to maximize or minimize the soil thrust on the wall depending on the limit state of interest (active or passive), Fig. 1a. Seeking an analytical solution without involving heuristic procedures such as those employed by Coulomb, Rankine [1] was the first to consider the limit stresses in the soil based on the principles of continuum mechanics i.e., by solving the pertinent differential equations of equilibrium in the backfill, while simultaneously satisfying the failure criterion and the stress boundary conditions. Using this approach and employing the so-called conjugate planes theorem, Rankine was able to solve the idealised case of an infinite slope of cohesionless soil (unit weight γ, friction angle φ) and demonstrate that the soil thrust on any vertical plane is parallel to the soil surface having an inclination equal to the backfill inclination, β, Fig. 1b. This suggests that the Rankine solution for a vertical wall is limited to the case where the wall roughness is equal to the backfill inclination. However, the generalized problem treated by Coulomb's method, involving a wall of arbitrary roughness δ_w and inclination ω, was not addressed by Rankine. The effect of wall roughness in Rankine's analysis was later investigated by several researchers including Saint-Venant [10], Levy [11] and Boussinesq [12] - see review by Heyman [4].

* Corresponding author. Department of Civil Engineering, University of Bristol, Bristol, UK
E-mail addresses: p.kloukinas@greenwich.ac.uk (P. Kloukinas), g.mylonakis@bristol.ac.uk (G. Mylonakis).

https://doi.org/10.1016/j.soildyn.2024.108502
Received 25 November 2023; Received in revised form 17 January 2024; Accepted 17 January 2024
Available online 13 February 2024

Rankine's efforts to simultaneously satisfy equilibrium and the failure criterion without considering compatibility of deformations, paved the way for the development of slip-line theory [3,11–16]. Due to inherent difficulties in integrating the relevant non-linear governing equations for frictional materials [2,4,17], only a handful of exact closed-form solutions exist for cases encompassing soil self-weight. These solutions are typically associated with straight stress characteristics like those involved in the classical Rankine solution. Despite the idealised nature of these formulations, employing a uniform stress field in the backfill, associated with straight stress characteristics, to determine earth pressures is attractive as it greatly simplifies the analysis. In this context, Chu [18] extended the classical solution of Rankine to encompass inclined walls [19–22], while an extension pertaining to seismic conditions was later published by Iskander et al. [23]. Other approximate solutions for assessing seismic earth pressures using limit states and various elastoplastic methods have been proposed, among others, by Ebeling et al. [24], Kloukinas [25], Shamsabadi et al. [26], Xu et al. [27] and Conti & Caputo [58]. Various comparisons of the predictions of the methods against experimental measurements are available, including the studies by Giarlelis & Mylonakis [28] and Kloukinas et al. [29].

The classical Rankine solution considers the tractions on a vertical plane which act parallel to the soil surface. For a horizontal backfill, the tractions act horizontally; the active and passive Rankine earth pressure coefficients are then obtained from the familiar expressions $K_\gamma = (1 \mp sin\,\varphi)/(1 \mp sin\,\varphi)$ or $\tan^2(45 \mp \varphi/2)$, where the upper and lower signs correspond to active and passive conditions, respectively.

For a backfill inclined at an angle β, the Rankine earth pressure coefficients are obtained by Eq. (1) [30]

$$K_\gamma = cos\,\beta \frac{cos\,\beta \mp \sqrt{cos^2\,\beta - cos^2\,\varphi}}{cos\,\beta \pm \sqrt{cos^2\,\beta - cos^2\,\varphi}} \tag{1}$$

where, again, the upper sign in the numerator and the denominator corresponds to active conditions and the lower sign to passive.

The earth pressure coefficient derived by Chu [18] is provided by Eq. (2a) and the inclination of the soil thrust is specified by Eq. (2b)

$$K_\gamma = \frac{cos(\beta - \omega)\sqrt{1 + sin^2\,\varphi \mp 2\,sin^2\,\varphi\,cos\,\theta_{a,p}}}{cos^2\,\omega\left(cos\,\beta \pm \sqrt{cos^2\,\beta - cos^2\,\varphi}\right)} \tag{2a}$$

$$\delta_{a,p} = tan^{-1}\left[\frac{sin\,\varphi\,cos\,\theta_{a,p}}{1 \mp sin\,\varphi\,sin\,\theta_{a,p}}\right] \tag{2b}$$

where $\theta_{a,p} = sin^{-1}\,[sin\beta/sin\varphi] \mp (\beta - 2\omega)$, and the double sign has the same meaning as before.

It is noted that the inclination of soil thrust on the wall, $\delta_{a,p}$, in the above equations does not necessarily coincide with the actual roughness of the soil-wall interface δ_w (this is also true in the simple Rankine case $\delta_{a,p} = \beta$ that Eq. (2) reduces to for $\omega = 0$) and renders the whole approach dubious. Similar, yet correct, solutions for pseudo-dynamic seismic thrusts on semi-gravity (L-shaped) cantilever walls have been derived by Evangelista et al. [31] and Kloukinas & Mylonakis [32], employing a pair of slip planes of roughness equal to the soil friction angle. The validity and limitations of the generalized Rankine solutions are discussed herein with emphasis on key new results including analytical solutions for the critical values of backfill inclination, amplitude of seismic body forces, and the soil friction angle required to induce Rankine conditions. Some advantages and limitations of these solutions are presented here for the first time, with the help of parametric studies.

2. Generalized limit stress analysis

Limit stresses in the backfill are determined based on the infinite slope assumption shown in Fig. 2, which is asymptotically exact at large

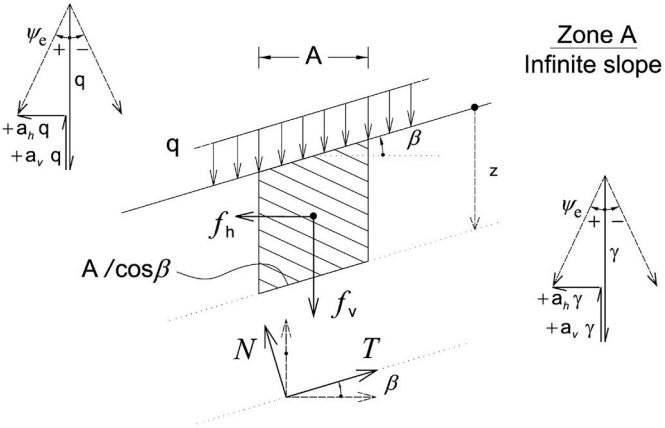

Fig. 2. Infinite slope equilibrium (Zone A), for combined gravitational and seismic action. Further, the normal and shear stresses (σ_β, τ_β) acting parallel to the soil surface are determined as linear functions of depth, yielding a constant stress ratio $(\tau_\beta/\sigma_\beta) = \tan(\beta + \psi_e)$, Eqs (3) and (4) .

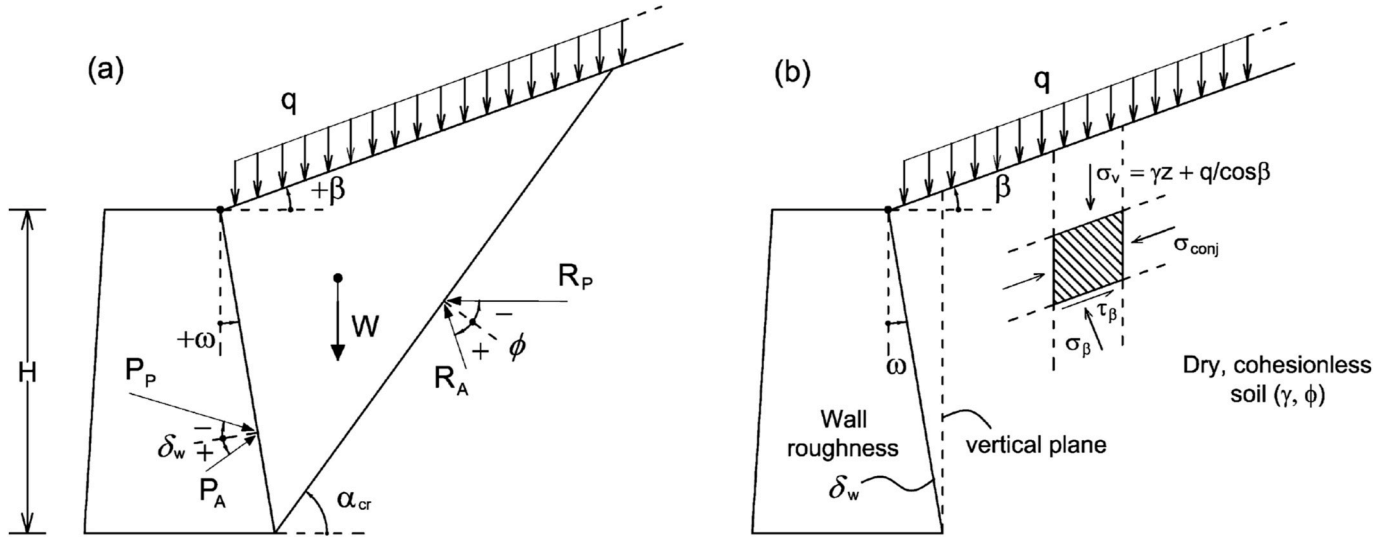

Fig. 1. (a) Coulomb's limit equilibrium wedge, (b) Rankine's conjugate stress planes approach.

distances from the wall [18,33–35]. Following the analysis presented in the above studies , the soil mass is assumed to be in a condition of limit equilibrium under the combined action of gravity and earthquake body forces with inclination $\psi_e = a_h/(1-a_v)$ (positive values pertaining to active conditions i.e., body forces pointing towards the wall). The same inclination is considered to also apply for the surcharge q, as a convenient but not necessary assumption since there is no rotational similarity transformation associated with the analysis at hand, like the one used for the non-Rankine stresses in Mylonakis et al. [35]. The contact tractions acting on the vertical sides of the soil element of Figs. 1 and 2, are mutually cancelling due to symmetry, so that the body forces $f_h = A\ \gamma\ z\ a_h$, $f_v = A\ \gamma\ z\ (1\ -\ a_v)$ and the corresponding force due the vertical surcharge $f_q = A/\cos\beta\ q\ (1\ -\ a_v)$ are in equilibrium with the reactions N and T at the base of the soil element, A being the arbitrary width of the element, Fig. 2.

$$\sigma_\beta = \frac{N}{A/\cos\beta} = \left(\gamma z + \frac{q}{\cos\beta}\right)(1-a_v)\cos^2\beta\cos(\beta+\psi_e)\ /\ (\cos\beta\cos\psi_e) \tag{3}$$

$$\tau_\beta = \frac{T}{A/\cos\beta} = \left(\gamma z + \frac{q}{\cos\beta}\right)(1-a_v)\cos^2\beta\ [\tan\beta + \tan\psi_e] \tag{4}$$

The position of the stress point $(\sigma_\beta, \tau_\beta)$ is shown on the Mohr circles of stresses in Fig. 3 for both active and passive conditions, as well as the corresponding position of the poles and the inclination of the major principal plane. Based on the geometry of the Mohr circle (Fig. 3a), the contact stress σ_θ acting on an arbitrary plane inclined by an angle θ with respect to the vertical can be related to the known stress point $(\sigma_\beta, \tau_\beta)$ through the mean stress S_A; the corresponding traction inclination (mobilised fiction) on this plane, $\delta_{m\theta}$, can also be calculated from the $(\tau_\theta/\sigma_\theta)$ ratio, as shown in Appendix B. These solutions are shown in Eqs. (5) and (6) below

$$\sigma_\theta = [1 - \sin\varphi\cos(\Delta_{2\theta} - \delta_{m\theta})]\ /\ [1 + \sin\varphi\cos(\Delta_{1e} + \beta + \psi_e)]\ \sigma_\beta \tag{5}$$

$$\tan\delta_{m\theta} = \tau_\theta/\sigma_\theta = [\sin\varphi\cos(\Delta_{2\theta} - \delta_{m\theta})]\ /\ [1 - \sin\varphi\cos(\Delta_{2\theta} - \delta_{m\theta})] \tag{6}$$

In the above expressions, $\Delta_{1e} = \sin^{-1}[\sin(\beta+\psi_e)/\sin\varphi]$ and $\Delta_2 = \sin^{-1}(\sin\delta_{m\theta}/\sin\varphi)$ denote the auxiliary Caquot angles shown on the Mohr circle diagrams of Fig. 3 [17,36]. Also, the term $\Delta_2 - \delta_{m\theta}$ in the above expressions can be replaced by the known quantity $(\Delta_{1e} - \beta + \psi_e + 2\theta)$ to simplify the analysis as shown in Mylonakis et al. [35].

Following the approaches available in literature, one can readily determine from the above stress fields the earth pressures on the wall plane, as well as the corresponding thrust inclination, treated as

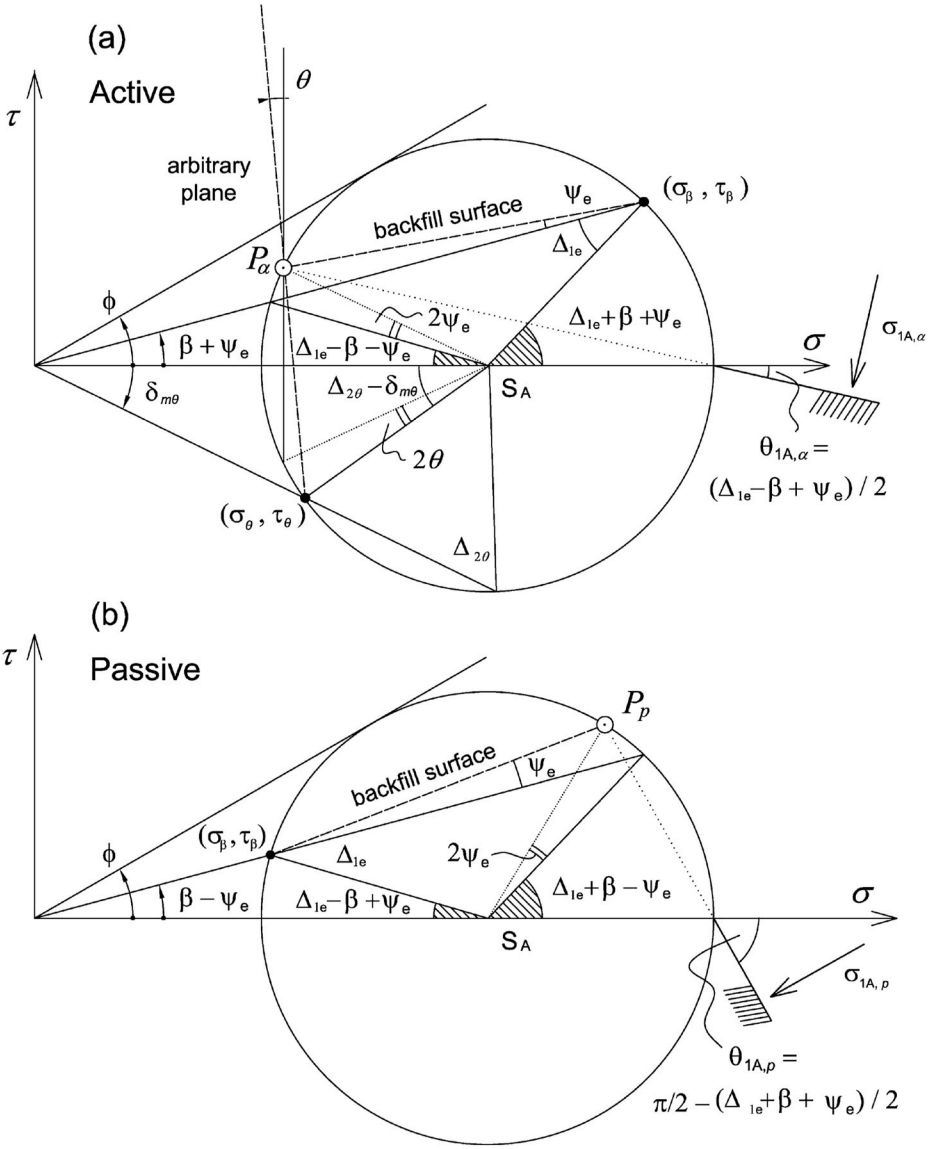

Fig. 3. Stress tensors near the backfill surface (Zona A) for active and passive conditions.

mobilised interface friction angles. This result, however, can be physically justified only in terms of a perfectly bonded interface, i.e. a static frictional mechanism which may not occur in practice. In other words, the soil-wall interface may instead turn into an actual sliding surface with peak shear resistance (friction angle δ_w) mobilised at lower strains relative to the friction angle φ of the backfill [37–39]. This is indeed the case, except for minor localization phenomena at the wall base, especially when rotational modes of failure are involved [37,40,41].

Moreover, the direction of the shear traction on the wall surface is governed by kinematic considerations that are not explicitly considered by stress solutions like the one at hand, and which are obviously different under active and passive conditions given the tendency of the backfill to move downward or upward, respectively, relative to the wall, Fig. 4. Evidence of the above can be found in the literature [37,40–45]. Evidently, contrary to common perception, stress solutions are not always independent of the kinematics of the problem and may require such information to make proper predictions [46].

The arising stress boundary condition according to the aforementioned physical restrictions enforces a boundary condition at the soil-wall interface of the form $\tau_w = \sigma_w \tan\delta_w$, where σ_w and τ_w are the normal and the shear component of contact traction, respectively, and specify the position of the stress point on the Mohr circle, which is different for active and passive conditions, as evident in Fig. 5 [25,35].

Accordingly, the stress states arising from the two boundary conditions are generally different unless the angle separating the two principal planes in Zones A (Fig. 3) and B (Fig. 5) is zero.

The above analysis yields the following solution for the normal traction on the wall

$$\sigma_w = S_B[1 - \sin\varphi\cos(\Delta_2 - \delta_w)] \tag{7}$$

where $\delta = \delta_w$ and Δ_2 is the corresponding Caquot angle

$$\Delta_2 = \sin^{-1}(\sin\delta_w / \sin\varphi) \tag{7b}$$

The inclination of the major principal plane from the horizontal is $\theta_{1B,\alpha} = (\Delta_2 - \delta_w - 2\omega)/2$, Fig. 5. In the general case, the principal planes and the corresponding stress characteristics in zones A and B, are separated by the angle θ_{AB} given by Eq. (8)

$$\theta_{AB} = \theta_B - \theta_{Ae} = [(\Delta_2 - \delta_w) - (\Delta_{1e} - \beta) - 2\omega - \psi_e]/2 \tag{8}$$

where, as discussed earlier,

$$\Delta_{1e} = \sin^{-1}[\sin(\beta + \psi_e)/\sin\varphi] \tag{8b}$$

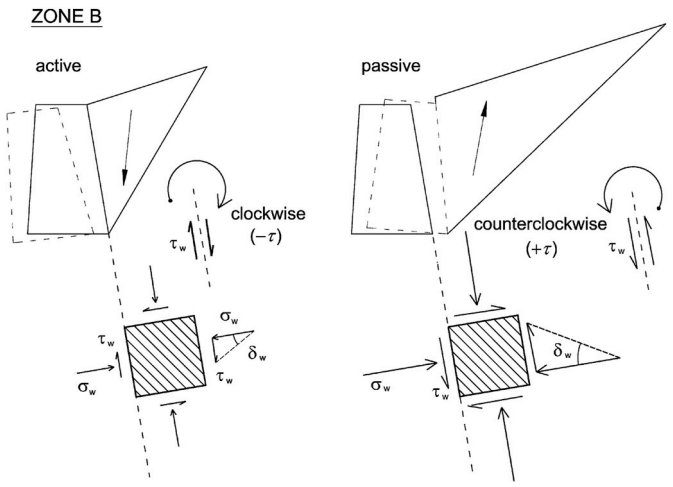

Fig. 4. Effect of kinematic conditions on the orientation of contact stresses for shear failure at the wall-soil interface (Zone B). [Positive notation shown follows the one adopted in this work.].

is a second Caquot angle pertaining to Zone A.

In the special case at hand of a vanishing angle θ_{AB} (Rankine state), one obtains the condition

$$(\Delta_2 - \delta_w) - (\Delta_{1e} - \beta) - 2\omega - \psi_e = 0 \tag{9}$$

Also, the overall seismic thrust on the wall can be obtained by integrating Eq. (5) along the surface of the wall to get

$$P = \int_0^{H/\cos\omega} p\,ds = \int_0^{H/\cos\omega} \frac{\sigma_w}{\cos\delta_w} ds \tag{10}$$

Introducing the change of variables (Fig. 6),

$$z = h\ (1 + \tan\omega\tan\beta) = h\cos(\omega - \beta)/[\cos\omega\cos\beta] \tag{11a}$$

and noting that

$$ds = dh/\cos\omega \tag{11b}$$

yields the following exact solution for the limit (active or passive) thrust

$$P_E = K_{qE}(1 - a_v)qH + \frac{1}{2}K_{\gamma E}(1 - a_v)\gamma H^2 \tag{12}$$

where,

$$K_{\gamma E} = \frac{\cos(\omega - \beta)\cos(\beta + \psi_e)}{\cos\delta_w\cos^2\omega\cos\psi_e}\left[\frac{1 - \sin\varphi\cos(\Delta_2 - \delta_w)}{1 + \sin\varphi\cos(\Delta_{1e} + \beta + \psi_e)}\right] \tag{13}$$

$$K_{qE} = K_{\gamma E}\frac{\cos\omega}{\cos(\omega - \beta)} \tag{14}$$

are the corresponding earth pressure coefficients due to self-weight and surcharge.

It is important to stress that Eqs. (13) and (14) are symmetric in the sense they can provide both active and passive limit states for proper values of the soil and interface friction angles φ and δ_w, as well as seismic action angle ψ_e (i.e., positive δ_w, φ, ψ_e for active conditions and negative δ_w, φ, ψ_e for passive). Further, for the Rankine case at hand the term $(\Delta_2 - \delta_w)$ in the numerator of Eq. (13) can be replaced with $(\Delta_{1e} - \beta + 2\omega + \psi_e)$ by means of Eq. (9), to simplify calculations. Similar formulations, for the gravitational case - without integrating the contact stresses, are given by Caquot & Kerisel [36], Costet & Sanglerat [47] and Soubra [48].

Alternative expressions have been derived by Chu [18] and Iskander et al. [23], which, however, are complicated and not symmetric with respect to active and passive conditions, involving square root terms that become indeterminate upon a change in sign of parameters δ_w, φ, and ψ_e.

3. Parametric analysis of the generalized Rankine stress condition

The Rankine condition in Eq. (9) can be satisfied by infinite combinations of the five governing parameters φ, δ_w, ω, β and ψ_e. Among them are the familiar cases $\delta_w = \omega = \beta = \psi_e = 0$ (i.e., vertical smooth wall, horizontal backfill) and $\delta_w = \beta$, $\omega = \psi_e = 0$ (vertical rough wall of roughness equal to the slope inclination). It is also straightforward to solve Eq. (9) with respect to each of the above parameters as function of the others to get Eqs (15)–(19).

$$\omega_R = \frac{1}{2}[(\Delta_2 - \delta_w) - (\Delta_{1e} - \beta) - \psi_e] \tag{15}$$

$$\delta_R = \tan^{-1}\left[\frac{\sin\varphi\sin(\Delta_{1e} - \beta + \psi_e + 2\omega)}{1 - \sin\varphi\cos(\Delta_{1e} - \beta + \psi_e + 2\omega)}\right] \tag{16}$$

$$\beta_R = \tan^{-1}\left[\frac{\sin\varphi\sin(\Delta_2 - \delta_w - 2\omega - 2\psi_e)}{1 - \sin\varphi\cos(\Delta_2 - \delta_w - 2\omega - 2\psi_e)}\right] - \psi_e \tag{17}$$

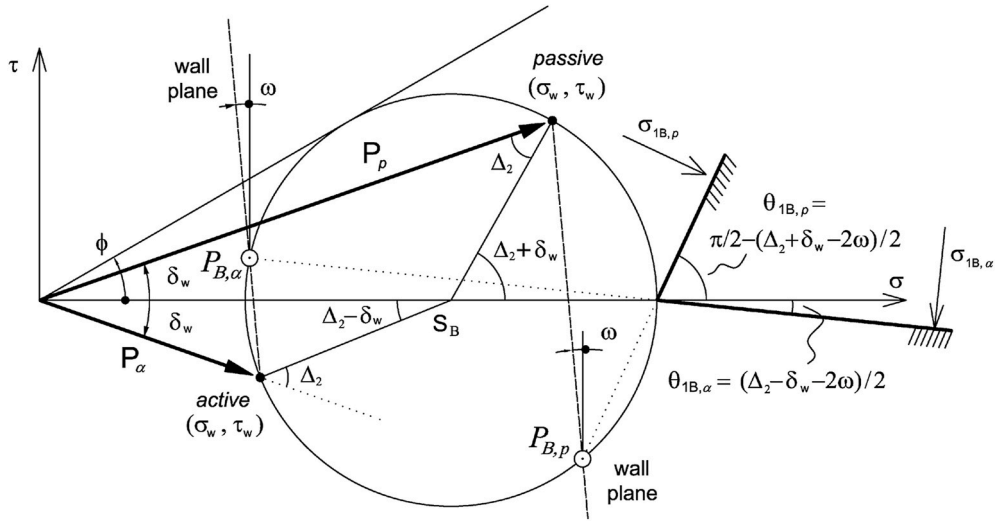

Fig. 5. Active and passive conditions calculated from the stress tensor in the vicinity of the wall (Zone B). The arrows in bold denote the corresponding tractions on the wall.

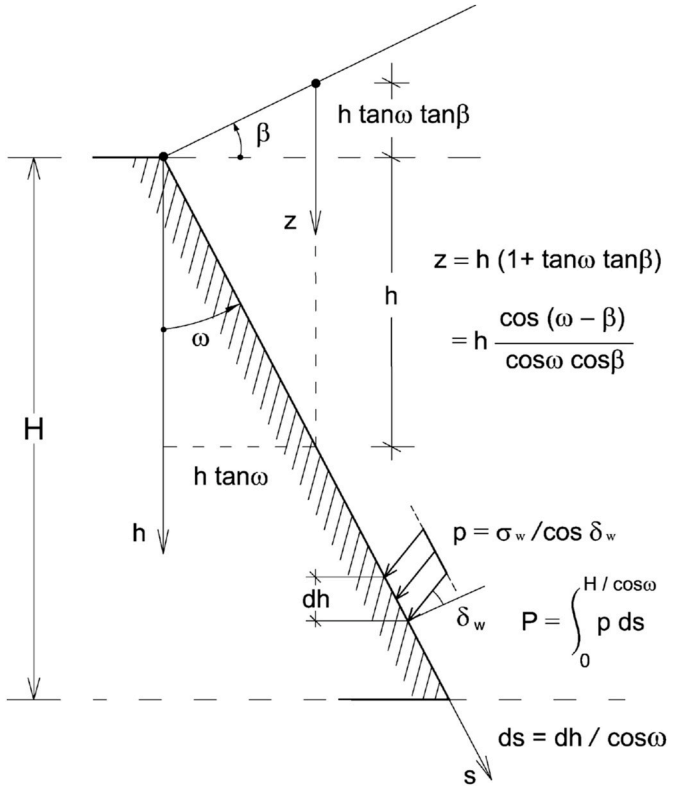

Fig. 6. Integration of contact stresses along the wall surface.

$$\psi_{eR} = tan^{-1}\left[\frac{sin\,\varphi\,sin(\Delta_2 - \delta_w - 2\omega + 2\beta)}{1 + sin\,\varphi\,cos(\Delta_2 - \delta_w - 2\omega + 2\beta)}\right] - \beta \tag{18}$$

$$\varphi_R = sin^{-1}\left[\frac{\sqrt{sin^2\delta_w + sin^2(\beta+\psi_e) - 2sin\,\delta_w\,sin(\beta+\psi_e)cos(\delta_w - \beta + \psi_e + 2\omega)}}{sin(\delta_w - \beta + \psi_e + 2\omega)}\right] \tag{19}$$

It should be noted that Equation (15) results directly from Eq. (9), whereas derivation of Eqs. (16)–(19) requires some algebraic manipulations provided in Appendix B.

For purely gravitational loading ($\psi_e = 0$), the counterparts of Eqs. (15) and (16) can be found in the works of Levy [11], Saint-Venant [10], Considère [49], Caquot & Kerisel [36], Costet & Sanglerat [47] and Chu [18], whereas more complicated alternatives to Eq (16) have been derived by Evangelista et al. [31] and Iskander et al. [23]. Equations (17)–(19) were derived in the PhD dissertation of Kloukinas [25] and are presented here for the first time.

Eq. (19) provides unique friction angle values φ that satisfy Eq. (9), except for some special cases where Eq. (19) becomes indeterminate and Eq. (9) is satisfied for all values of φ. Among these are the classical Rankine conditions ($\delta_w = \omega = \beta = \psi_e = 0$; $\delta_w = \beta$, $\omega = \psi_e = 0$), or the case where $\delta_w = \beta + \psi_e$ and $\omega = -\psi_e$, which is an extension of Rankine's conjugate plane theorem for the seismic case. It is worth noting that some of the above equations have been explored in the past under different forms. The first investigations of the generalized Rankine solution were carried out in the 19th century by Saint Venant (1870), Considère [49] and Levy [11], who derived a simplified form of Eq. (15) and proposed that retaining walls should be designed with specific inclination so that the Rankine condition is met [4].

For the simpler case of gravitational loading, Eqs. (15) and (16) have been derived in a number of studies including Caquot & Kerisel [36], Costet & Sanglerat [47] and Chu [18]. As already mentioned, some of these solutions do not employ the predicted interface friction angles as actual (required) values, but merely as mobilised quantities on the surface of the wall - irrespective of the actual wall roughness δ_w, without even discussing the sign of the predicted interface friction angle [21]. Accordingly, these solutions may violate the failure criterion on the wall-soil interface and are often incompatible with the kinematics of the problem, especially under passive conditions [18].

The above observations can be demonstrated with the help of experimental data. To this end, Fig. 7 depicts results from the experimental study of Fang et al. [50] for the active and passive thrusts developing on a vertical wall of roughness $\delta_w = 19.1°$ supporting a loose cohesionless backfill of friction angle $\varphi = 30.9°$ for different backfill inclinations i (same as symbol β in this work). The experimental results are compared against the predictions of some classical formulations, including the Rankine solution under the assumption $\delta_w = i$. The lower-bound type solution of Mylonakis et al. [35] has been included on the graphs for comparison. As evident from the plots, realistic Rankine conditions result only when the backfill inclination i is equal to the actual wall roughness δ_w, which corresponds to $\delta = i = \delta_w = 19.1°$ and different directions for the active and passive case. At parameter combinations where the Rankine condition is satisfied, the predictions of all solutions not only coincide, but are also exact in the realm of limit

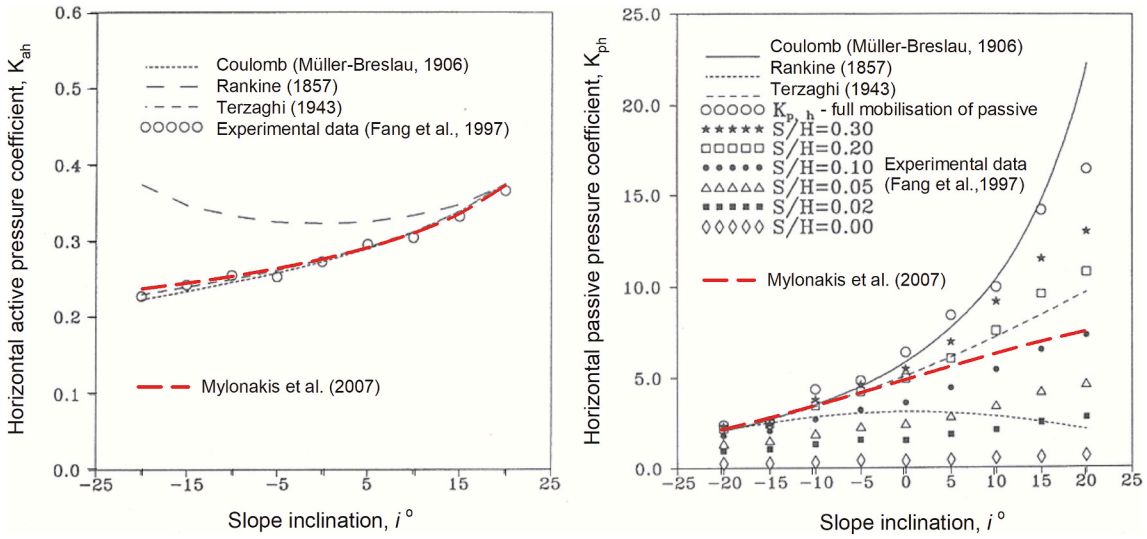

Fig. 7. Comparison of predictions for active and passive thrust, by various methods with experimental data by Fang et al. (*S/H* denotes horizontal wall movement over wall height.)

analysis, being in excellent agreement with the experimental measurements [18,20]. This can be attributed to the development of straight stress characteristics in the backfill which define the Rankine stress state. For other points in the graphs, the stress characteristics are generally curved to satisfy the (incompatible) inclinations of the major principal planes close to the wall and the soil surface. Evidently, the Rankine solution is conservative for both active and passive conditions on these plots.

Results for the critical wall inclination ω_R based on Eq. (15) are depicted in Fig. 8 (plotted in terms of the ratio ω_R/φ) for purely gravitational loading ($\psi_e = 0$), as a function of the soil friction angle φ and different backfill inclinations β/φ. Wall roughness $\delta_w/\varphi = 1/2$ is assumed in all plots. Apart from the special case of a vertical wall ($\omega_R = 0$) where classical Rankine conditions develop for $\delta_w = \beta$, generalized Rankine conditions could be readily fulfilled in the active case for positive backfill inclinations ($\beta > 0$) and in the passive case for negative inclinations ($\beta < 0$).

Otherwise, very large (unfeasible) wall inclinations would be required, especially in the passive case. Further, an increase in wall roughness (not shown here in the interest of space) would lead to an increase in critical wall inclination ω_R for both active and passive conditions. As visible in the graphs on the left side, for $\varphi = 35^\circ$ to 40° the critical wall inclination for a horizontal backfill under purely gravitational loading is on the order of 10° and 30° for active and passive conditions, respectively.

Fig. 9 presents the same solution with the inclusion of earthquake acceleration $a_h = 0.2$ g and two different wall roughness values, $\delta/\varphi = 1/2$ and 2/3. The results indicate a significant reduction in critical wall inclination ω_R both for active and passive conditions, with the reduction being stronger for the passive case. An increase in wall roughness would, again, lead to an increase in critical wall inclination for both active and passive conditions.

Results for the critical wall roughness δ_R under pure gravitational loading are presented on Table 1 for different backfill inclinations β, different wall inclinations ω, and different friction angles φ. Based on these results, the critical wall roughness coincides with the backfill inclination only when the wall is vertical ($\omega = 0$). These results may lead to unfeasible roughness values that are incompatible with the kinematics of the problem which dictate the direction of shear tractions on the wall surface. For this reason, the negative and positive values obtained for active and passive conditions respectively, are denoted with an asterisk because they correspond to kinematically inadmissible states. The specific physical constraint is often not acknowledged in the literature (e.g. Ref. [18]) where such values are provided without discussion. The influence of soil friction angle φ on wall roughness for inclined walls and a symmetrical condition between the ratios β/φ and ω/φ are also evident on Table 1. Finally, it appears that the Rankine condition is mostly feasible for positive wall inclinations, especially for the active case, while for the passive case the Rankine condition is unfeasible for large positive values of ω and all physically realizable values of wall roughness.

In Fig. 10, the effect of earthquake action on the critical wall roughness, δ_w, is examined for a horizontal acceleration $a_h = 0.2$, for the same cases investigated in Table 1 and a vertical wall ($\omega = 0$). Evidently, the critical wall roughness under earthquake action is not equal to the slope inclination β as in the classical Rankine solution, but increases for both active and passive conditions, approaching the limit value $\delta_w = \varphi$ for relatively steep backfills and high friction angles φ. Remarkably, the active Rankine state is feasible under earthquake action even for negative slope angles ($\beta < 0$), whereas the passive state might not be feasible for $\beta > 0$, as this would require positive values of δ_w which are not physically admissible for the specific limit state.

The amplitude of seismic acceleration α_h required to ensure a Rankine stress state in depicted in Fig. 11 for a vertical smooth wall ($\omega = \delta_w = 0$), negative slope inclination ($\beta < 0$) for the active case and positive inclination ($\beta > 0$) for the passive. As evident from the graphs, α_h values fall into a reasonable range only for the active case (up to 0.15g), whereas for the passive case extreme accelerations are needed (up to 2g), especially for steep and dense backfills. For opposite backfill inclinations ($\beta > 0$ for active and $\beta < 0$ for passive), the results indicate non-critical orientation of the seismic action, that is seismic action pointing towards the backfill in the active case and towards the wall in the passive.

An additional parametric investigation is presented in Fig. 12, in terms of the critical wall roughness for different seismic accelerations and backfill inclinations. In accordance with the aforementioned observations, passive Rankine conditions are feasible for negative backfill inclinations ($\beta < 0$) with only minor influence of seismic acceleration level. On the other hand, wall inclination has a stronger effect on δ_R, which results in a wider range of roughness values. Active Rankine conditions are fulfilled for all backfill inclinations, even negative ones. For an inclined wall ($\omega = 20^\circ$), the active Rankine condition requires high wall roughness corresponding to a δ_w/φ ratio of almost 1.

Fig. 13 explores conservatism aspects of the generalized Rankine solution for a vertical wall of natural roughness $\delta = 0$ or $\delta = 15^\circ$ retaining a backfill of $\varphi = 30^\circ$ and variable inclination β, subjected to purely gravitational loading ($\psi_e = 0$). Both active and passive states are

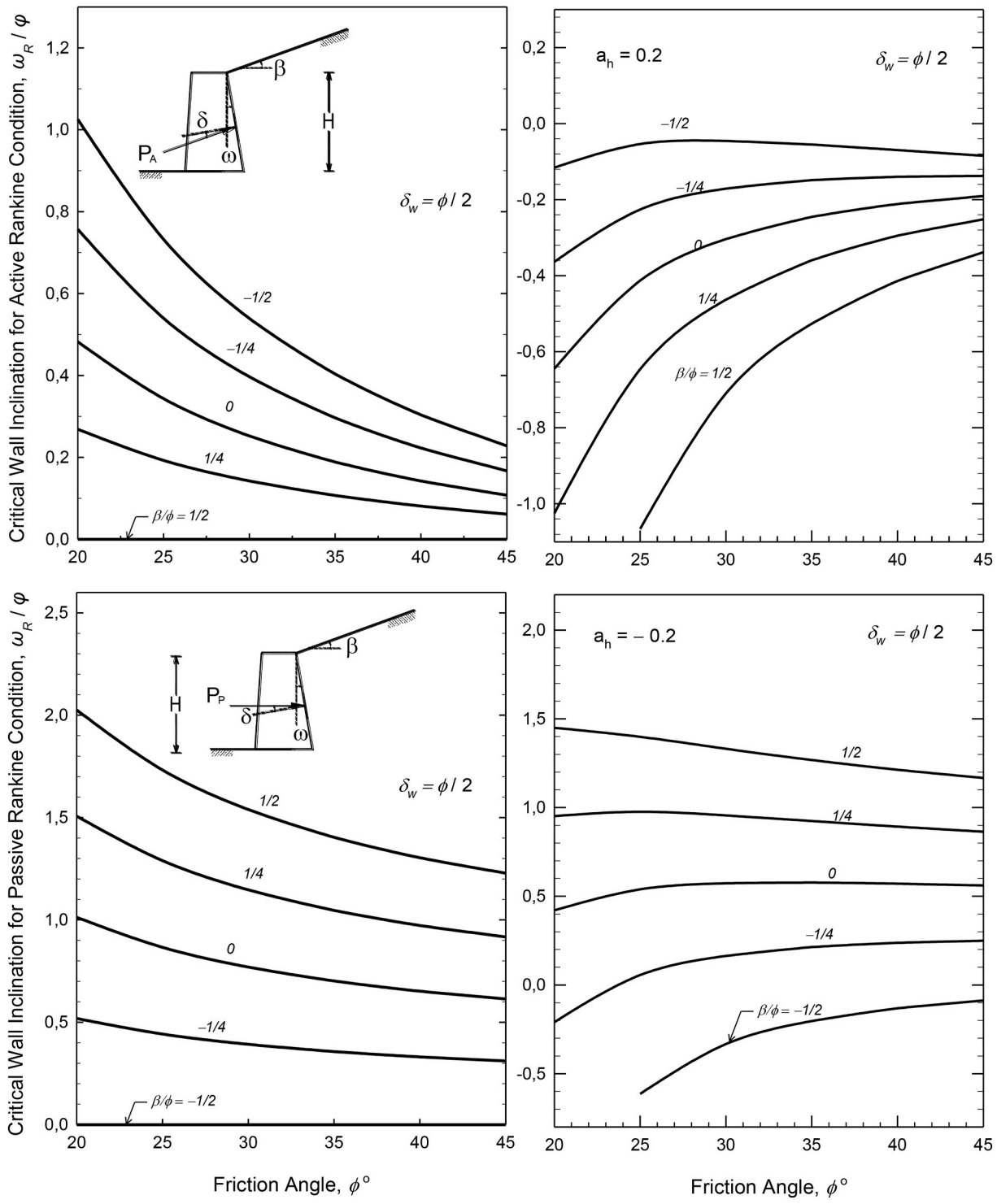

Fig. 8. Variation of critical wall inclination under gravitational loading to fulfill the generalized Rankine condition as function of soil friction angle φ, for different backfill inclinations β; $\delta_w = \varphi/2$.

explored. The predictions of the general stress solution (a conservative formulation) by Mylonakis et al. [35] and the classical limit-equilibrium solution (an unconservative formulation) by Coulomb/Müller-Breslau, are included in the graphs for comparison, under the assumption $\delta = \delta_w$. Ten (10) slope inclinations β (equal to the critical Rankine wall roughness δ_R) are considered, varying from -25° to $+25^\circ$. The predictions of all three methods coincide for the correct slope inclination/wall roughness $\beta\ (=\delta) = \delta_w$ and deviate away from that value, with the stress solution being always on the conservative side relative to the limit equilibrium solution.

It should be noted that the predictions of the Rankine solution for the vertical wall and purely gravitational loading at hand are meaningful only when: (1) the mobilised roughness δ_R (or slope inclination $\beta = \delta_R$) are positive for active conditions and negative for passive; (2) the mobilised roughness δ_R is smaller (or equal), in absolute terms, than the actual wall roughness δ_w. If both these conditions are met, the Rankine solution will be conservative (or exact if $\delta_R = \delta_w$) as evident on the upper right graph for $0 < \delta_R < 15^\circ$, the lower right graph for $-15^\circ < \delta_R < 0$,

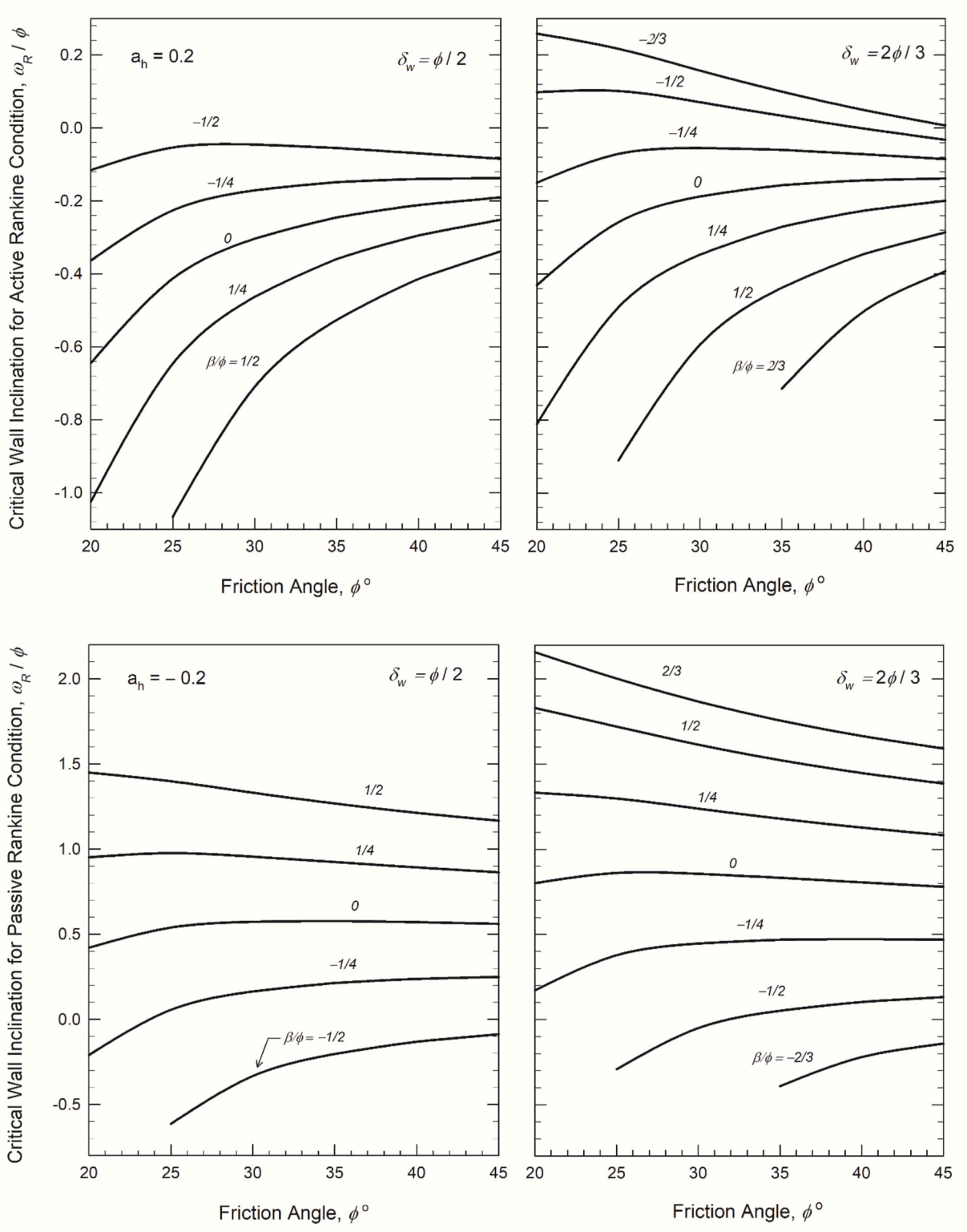

Fig. 9. Variation of critical wall inclination to fulfill the generalized Rankine condition as function of friction angle φ, for different backfill inclinations β and horizontal earthquake action $a_h = 0.2$, $\delta_w = \varphi/2$ and $2\varphi/3$.

and the graphs on the left side for $\delta_R = 0$. Interestingly, for the two graphs on the left side the only valid roughness value is $\delta_R = 0$, as for higher or lower values the solution will either violate the failure criterion on the wall, or be unfeasible from a kinematic viewpoint. Evidently, outside its range of applicability, the generalized Rankine solution may be conservative or unconservative depending on the circumstances.

It is also noted in passing that in the region beyond $\beta = 15°$ where all methods seem to provide the same overall soil thrusts (upper right graph), the Rankine solution employs a higher backfill inclination (recall that $\beta = \delta_R$), so the horizontal component of soil thrust drops (while the vertical component increases), which renders the Rankine solution gradually less conservative. This is further discussed in the

Table 1
Critical wall roughness δ_R/φ for active and passive conditions under gravitational loading.

β/φ		-½			-¼			0			¼			½		
ω/φ		-½	0	½	-½	0	½	-½	0	½	-½	0	½	-½	0	½
col #		{1}	{2}	{3}	{4}	{5}	{6}	{7}	{8}	{9}	{10}	{11}	{12}	{13}	{14}	{15}
φ^o -	25°	-{15}	−0.5	0.194	-{12}	−0.25	0.452	-{9}	0	0.646	-{6}	0.25	0.795	-{3}	0.5	0.909
Active	30°	(*)	(*)	0.436	(*)	(*)	0.650	(*)		0.793	(*)		0.894	(*)		0.963
	35°			0.679			0.823			0.909			0.963			0.994
	40°			0.871			0.942			0.979			0.996			0.999
	45°			0.975			0.995			1.000			0.996			0.983
φ^o -	25°	−0.216	−0.5	−0.750	-{12}	−0.25	−0.531	-{9}	0	−0.294	-{6}	0.25	−0.045	-{3}	0.5	-{1}
Passive	30°	−0.179		−0.782	(*)		−0.565	(*)		−0.330	(*)	(*)	−0.082	(*)	(*)	(*)
	35°	−0.147		−0.809			−0.595			−0.360			−0.113			
	40°	−0.119		−0.834			−0.621			−0.387			−0.140			
	45°	−0.094		−0.856			−0.644			−0.410			−0.163			

(*) Unfeasible.

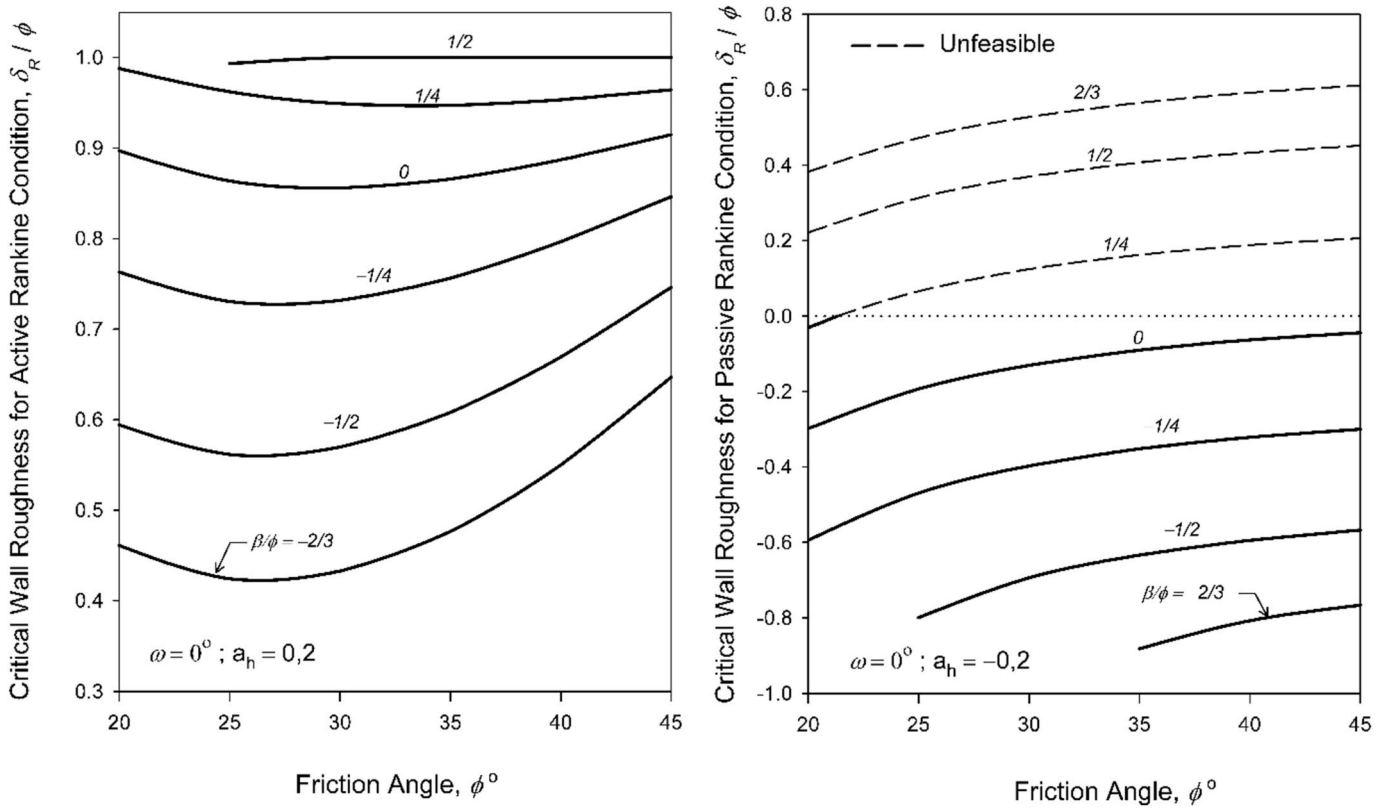

Fig. 10. Variation of critical wall roughness to fulfill the generalized Rankine condition, as function of friction angle φ, for different backfill inclinations β, vertical wall and horizontal earthquake action $a_h = 0.2$.

numerical example in Appendix A.

A graphical summary of the behavior of the generalized Rankine solution from the viewpoint of feasibility and conservatism is provided in Fig. 14. The sketch shows how the physical restrictions as to the kinematics of the problem and the failure criterion on the soil-wall interface are affecting the conservatism of the solution and restricting its applicability. The following are worthy of note.

(1) The Rankine solution would be exact in the realm of limit analysis, mobilising the full strength of the soil-wall interface (and thus inducing a limit state in the backfill), only when $\delta_R = +\delta_w$ or $-\delta_w$ for active and passive conditions, respectively.
(2) The solution would remain meaningful when $0 < \delta_R < +\delta_w$ for active conditions and $-\delta_w < \delta_R < 0$ for passive (roughness points located within the base of the two large right triangles, Fig. 14). If these conditions are met, the solution is both physically realisable and conservative, and reaches a maximum level of conservatism for $\delta_R = 0$ (white circle at triangles top, Fig. 14). Nevertheless, it won't correspond to a true active or passive limit state, as the strength of the wall surface won't be exhausted.
(3) On the other hand, if the failure criterion on the wall is violated $|\delta_R| > |\delta_w|$ but the thrust inclination has the proper sign (i.e. positive roughness larger than $+\delta_w$ or negative roughness smaller than $-\delta_w$), the solution will turn unconservative and become most unconservative for $|\delta_R| = \varphi$ (white circles in small triangles, Fig. 14). In this range the solution will cease to be meaningful.
(4) If the Rankine wall roughness changes sign i.e. turns negative for active conditions or positive for passive (points along the broken lines above the triangles top), the solution will become even more conservative, yet unfeasible from a kinematic viewpoint.

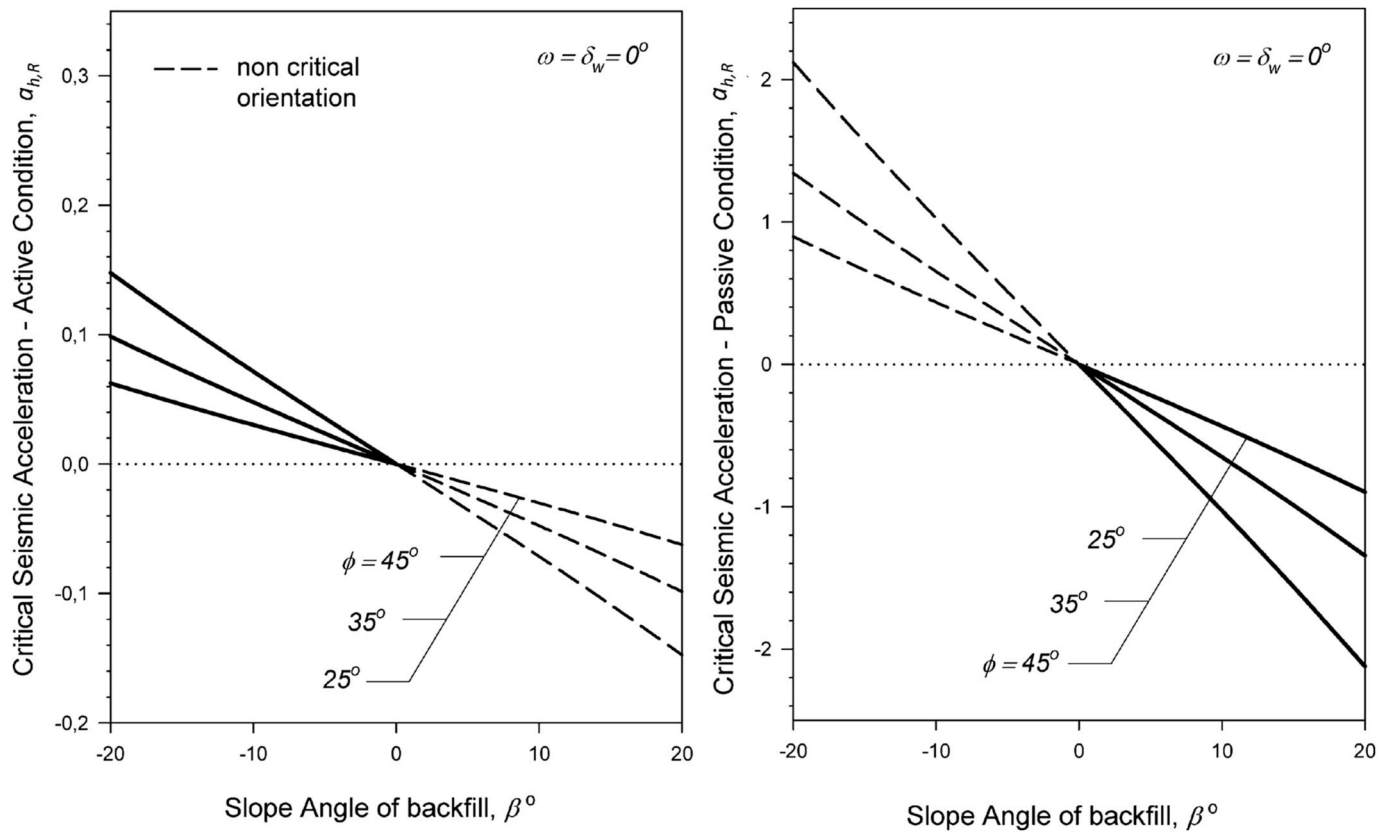

Fig. 11. Variation of critical earthquake acceleration to fulfill the generalized Rankine condition, as function of backfill inclination and friction angle φ, for a vertical smooth wall ($\delta_w = 0$).

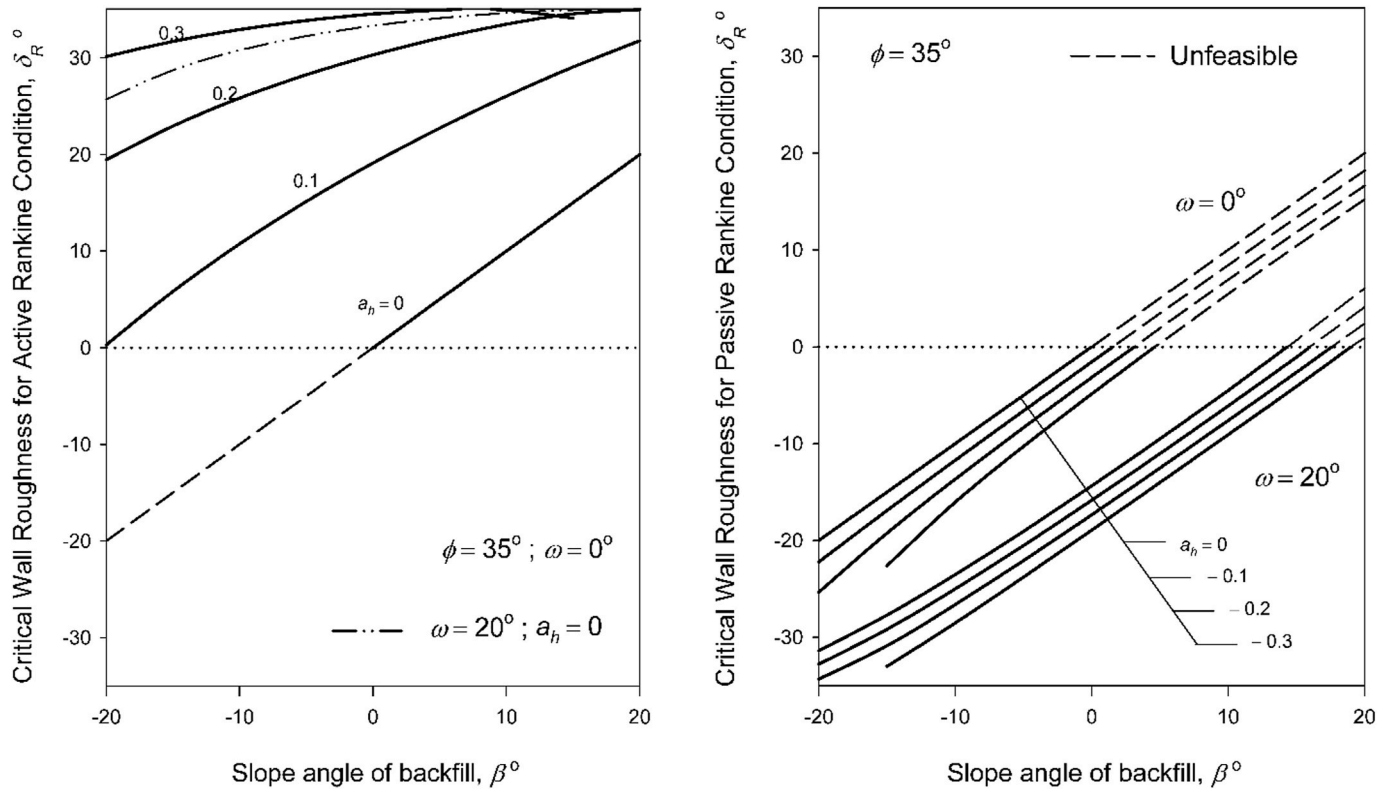

Fig. 12. Variation of critical wall roughness to fulfill the generalized active Rankine condition, as function of backfill inclination and horizontal earthquake acceleration for friction angle $\varphi = 35^o$ and wall inclination $\omega = 0$ and 20^o.

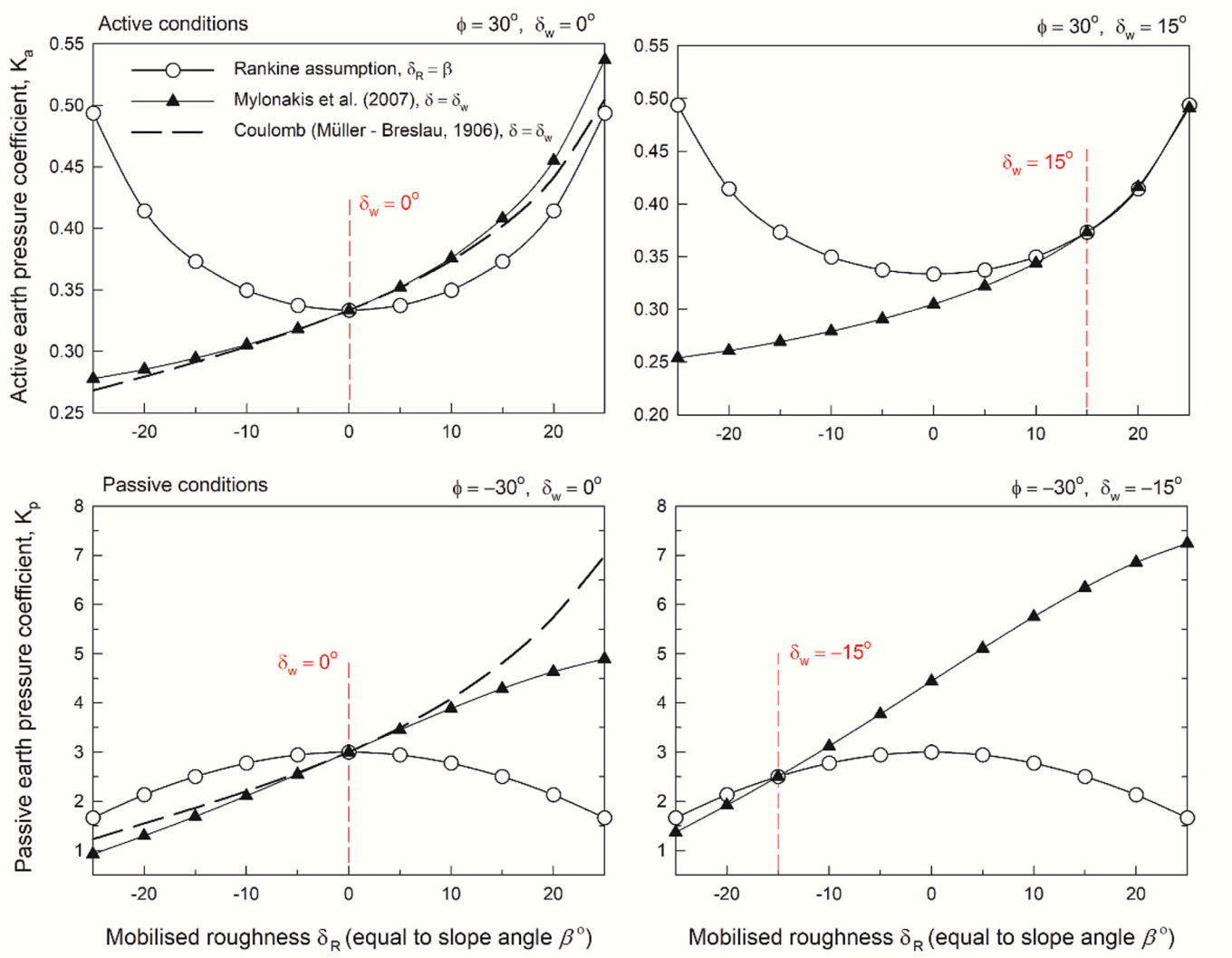

Fig. 13. Investigation of the conservatism of the Rankine solution relative to two general stress and limit equilibrium solutions for active and passive states under purely gravitational loading and a vertical wall; $\psi_e = 0$, $\omega = 0$, $\delta_w = 0$ (left) and $\delta_w = 15^\circ$ (right), $\varphi = 30.^\circ$

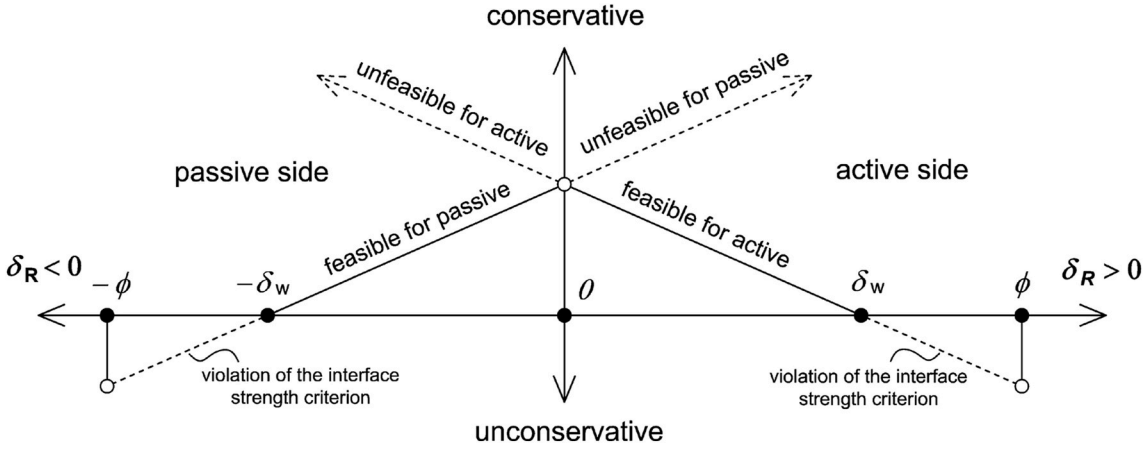

Fig. 14. Schematic of the behavior of the generalized Rankine solution in terms of conservatism (vertical axis) as a function of the relative values of the mobilised thrust inclination δ_R and the actual wall roughness δ_w (horizontal axis) for active and passive conditions.

It should be noted that the different possibilities in the predictions of the generalized Rankine solution as to the critical values of wall roughness δ_R can be explained considering that the strain-strain relations, displacement boundary conditions and compatibility of deformations are ignored in stress solutions.

4. Application of Rankine theory on cantilever walls

The aforementioned restrictions in the application of the generalized Rankine theory to conventional gravity walls disappear when the soil-wall interface is not part of the failure mechanism. This is the case

with the popular L-shaped cantilever walls (or semi-gravity walls) where the stress characteristics from the Rankine stress field of the retained mass (Zone A) do not intersect the stem of the wall, so the sliding prism is formed entirely in the backfill (Fig. 15). To fulfil this requirement, the inclination of the β -characteristic ω_β simply needs to satisfy the geometric requirement $\omega_\beta > \omega_{wall}$ [20,51]. The inclination of the β-characteristic for seismic conditions can be determined either graphically from the Mohr circle of Fig. 3 or, alternatively, from Eq. (15) using $\delta = \varphi$, to get

$$\omega_\beta = \frac{\pi}{4} - \frac{\varphi}{2} - \frac{\Delta_{1e} - \beta}{2} - \frac{\psi_e}{2} \tag{20}$$

The inclination ω_β naturally depends on the seismic angle ψ_e and tends to decrease with increasing acceleration, allowing application of the generalized Rankine theory even at walls with short heels that don't satisfy this geometrical requirement under static conditions [31,32].

Following common practice, earth pressures are calculated on a computational plane in the soil mass, commonly called the "virtual wall back". This can be any arbitrary plane inclined at an angle ω from the vertical, however, it is usually preferable to adopt the conventional vertical plane ($\omega = 0$), for it leads to a simpler geometry and equations [20,51]. Of fundamental importance in the virtual back approach [20,52,53] is the proper traction inclination to be considered on this plane, for which different approaches have been proposed, including $\delta = \beta$ (roughness equal to slope inclination according to the classical Rankine solution), $\delta = \delta_w$ (roughness equal to the actual soil-wall interface

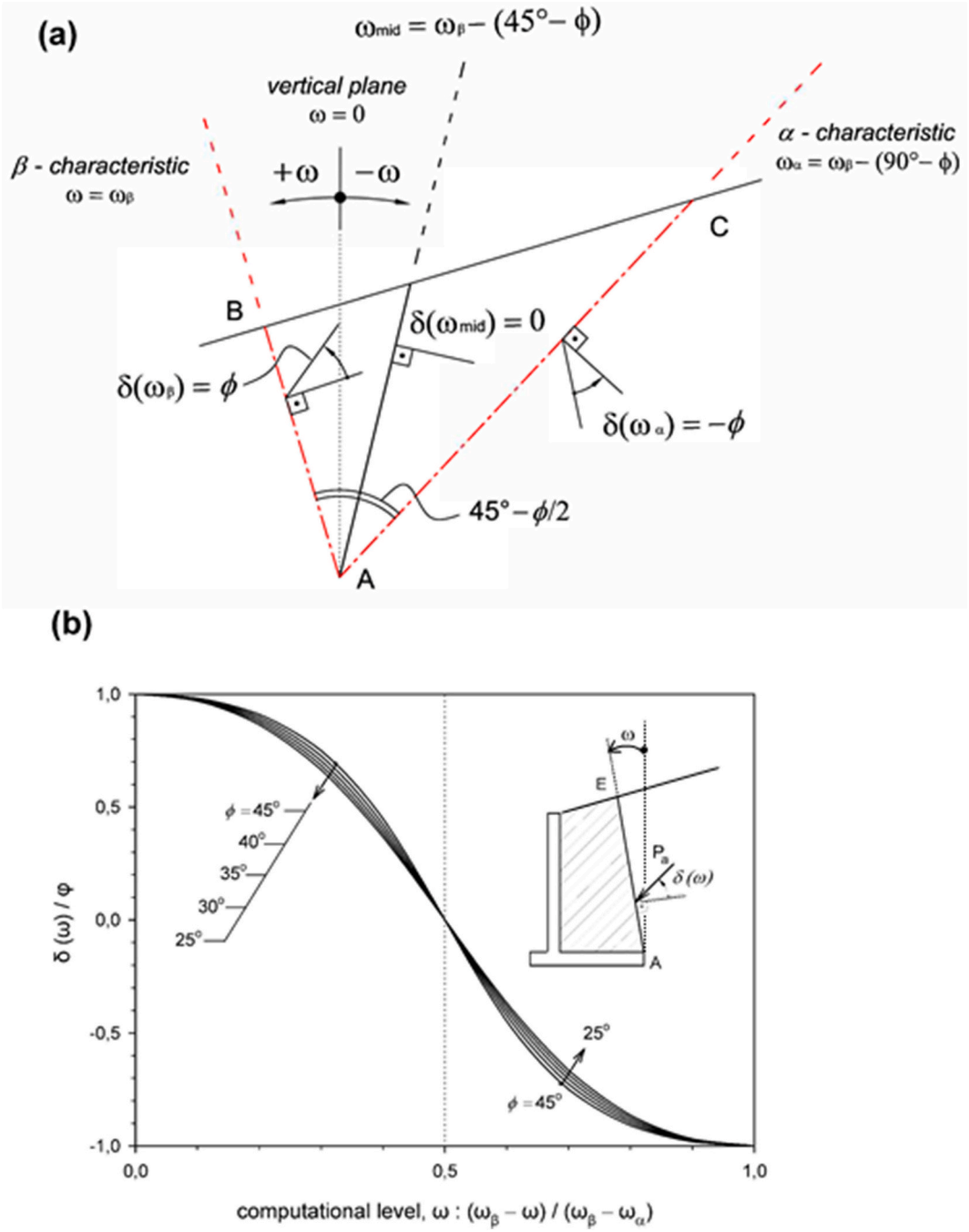

Fig. 15. (a) Extreme values of the inclination $\delta(\omega) = \pm\varphi$ on the boundaries of the Rankine failure prism, and (b) Variation of the dimensionless inclination $\delta(\omega)/\varphi$ across the Rankine prism (from ω_β to ω_a), for friction angles φ ranging from 25° to 45°.

roughness) and $\delta = \varphi$ (roughness equal to soil friction angle following a "soil-to-soil" friction assumption). Based on the generalized Rankine solution presented herein, the mobilised traction inclination on any arbitrary plane ω can be easily calculated from Eq. (6).

The variation of $\delta(\omega)$ across the whole Rankine wedge (from ω_β to ω_a) is depicted in Fig. 15, for friction angles varying from 25° to 45°. Naturally $\delta(\omega)$ is bounded between $-\varphi$ and $+\varphi$, which are the maximum possible mobilised values along the α- and β-characteristics. Using this mobilised value $\delta(\omega)$ in Eq. (5), the earth pressure on any selected plane can be established. Despite the variation of the amplitudes of active thrusts P_A and obliquities $\delta(\omega)$ depending on the selection of plane ω, it can be shown that all selections lead to statically equivalent systems, provided that the body forces in the corresponding hatched soil prism in Fig. 15 are accounted for [32].

Further, it can be shown that using the mobilised roughness $\delta(\omega)$ on any selected plane, the predictions of the generalized Rankine solution and the M − O formula will coincide, which is consistent with observations from studies on gravitational loading [18,20].

Finally, on the classical "vertical virtual back" approach, the thrust inclination would be equal to the slope angle β for purely gravitational loading (i.e., the classical Rankine solution) and would increase with increasing seismic acceleration up to a maximum value $\delta = \varphi$ when the β-characteristic becomes vertical ($\omega_\beta = 0$). This increase in thrust inclination would be beneficial for wall stability due to the associated decrease in driving forces and increase in resisting ones [29].

5. Conclusions

The theoretical basis of a generalized Rankine condition in a retained frictional soil with inclined surface behind an inclined, rough retaining wall has been examined, leading to the following conclusions.

1) Rankine stress fields can be induced for any combination of the five governing parameters (φ, δ_w, ω, β, ψ_e) matching the stress boundary conditions of the problem, beyond the classical Rankine cases known in literature (i.e., $\delta_w = \omega = \beta = \psi_e = 0$ and $\delta_w = \beta$, $\omega = \psi_e = 0$). It was shown that this condition can arise for infinite combinations of geometric and material parameters obeying a transcendental equation in friction angle φ, wall inclination ω, backfill slope β, wall roughness δ_w and body force inclination ψ_e [Eqs. (9) and (15)]. The above parameters are not independent, as the critical value (referred herein to as the "Rankine value") for any of these can be derived as a function of the rest.
2) Exact closed form solutions were derived, for the first time, for the case of seismic loading, providing the critical value of each parameter to fulfil the Rankine condition as a function of the rest [Eqs. (16)–(19)]. It was shown that a generalized Rankine stress condition can be satisfied for a wide range of parameters in the active case, but is less feasible for the passive. There are also conditions where these relations yield values which are not acceptable from a physical/kinematic viewpoint.
3) For the generalized Rankine condition at hand, an exact plasticity solution was derived for the problem of soil with self-weight, which yields straight stress characteristics in the backfill. However, this solution is valid only for the special cases described by Eqs. (9) and (15)-(19) and cannot be used unconditionally as an earth pressure predictor. From this perspective, the various Rankine formulas proposed in the literature may violate the failure criterion at the soil-wall interface and, in some cases, even the problem kinematics.
4) Regarding the effect of wall roughness, the solution is physically meaningful only when $0 < \delta_R < +\delta_w$ for active conditions and $-\delta_w < \delta_R < 0$ for passive, as show in Fig. 14. If these conditions are met, the solution will be exact for $\delta_w = \delta_R$ (corresponding to a true limit state) and conservative for $|\delta_R| < |\delta_w|$ (without referring to true a limit state as the strength of the soil-wall interface won't be exhausted). The maximum level of conservatism will be reached for $\delta_R = 0$.
5) On the other hand, if the failure criterion on the wall surface is violated but the thrust inclination has the proper sign (i.e. positive roughness larger than $+\delta_w$ or negative roughness smaller than $-\delta_w$), the solution will turn unconservative and become most unconservative as $|\delta_R|$ approaches φ. In this range the solution would cease to be meaningful.
6) Further, if the sign of the thrust inclination is violated (i.e., turns negative for active conditions or positive for passive), but the failure criterion is not violated (i.e., $|\delta_R| < |\delta_w|$), the solution will further increase in conservatism but, again, become unfeasible from a kinematic viewpoint.
7) The different possibilities as to the values of critical wall roughness δ_R can be explained considering that the strain-strain relations, displacement boundary conditions and compatibility of deformations are ignored in deriving stress solutions like the one at hand.
8) In case of semi-gravity cantilever retaining walls, the Rankine solution can be widely applied, especially under seismic action. Using the Rankine solution, the popular "vertical virtual back" approach was modified by means of an acceleration-dependent soil thrust inclination. This was shown to be beneficial for the stability of the soil-wall system, reducing the horizontal component and increasing the vertical component of soil thrust under increasing seismic acceleration. More information on this type of analysis is provided in Kloukinas and Mylonakis [32].

As a final remark, it is fair to mention that for cases where SSI and site effects are important (e.g. flexible walls, rigid basement walls, propped walls, deep soil deposits), more recent approaches such as the kinematic theory of earth pressures [54–57] that relate earth pressures to relative soil-wall movements, have started being used instead of the traditional limit state solutions. Discussing these methods lies beyond the scope of this paper.

CRediT authorship contribution statement

Panos Kloukinas: Writing – original draft, Formal analysis, Conceptualization. **George Mylonakis:** Writing – original draft, Supervision, Methodology, Conceptualization.

Declaration of competing interest

The authors declare that they have no known competing financial interests or personal relationships that could have appeared to influence the work reported in this paper.

Data availability

No data was used for the research described in the article.

Acknowledgements

Partial funding for the completion of this work was received through the Khalifa University – FSU 2021–028 [Project Title: "Next Generation Framework for Seismic Design of Quay Walls"]. The Authors are grateful to Dr Elia Voyagaki for proofreading the final manuscript.

Appendix A. Application Example

Active and passive earth pressures are computed for a number of practical cases using the generalized Rankine assumption against the general stress solution by Mylonakis et al. [35].

Considering the example adopted in Mylonakis et al. [35] and Powrie [8] - a gravity wall of inclination $\omega = 5^o$ retaining an inclined dry, cohesionless backfill with $\varphi = 30^o$ and $\beta = 15^o$, subjected to horizontal seismic acceleration $a_h = 0.2$, and vertical acceleration $a_v = 0$. The physical interface roughness of the wall is $\delta_w = 20^o$ ($= 2/3\varphi$), a common design recommendation for concrete-soil interfaces.

A.1 Active limit state

Considering positive horizontal acceleration $a_h = 0.2$ (i.e. pointing towards the wall) and $a_v = 0$.

- The general stress solution by Mylonakis et al. [35] predicts an active pressure coefficient $K_a = 0.816$, which can be decomposed into a horizontal component $K_{ah} = 0.740$ and a vertical component $K_{av} = 0.345$.
- The Rankine solution yields $\delta_R = 26.7^o$ (Eq. (16)) and $K_a = 0.846$ (Eq. (13)); the latter can be decomposed into a horizontal component $K_{ah} = 0.696$ and a vertical $K_{av} = 0.480$.

The following observations are worthy of note: *First*, the critical Rankine wall roughness of 26.7° is higher than the physical friction angle of the interface of 20°. Even though the overall earth pressure is higher relative to the general solution (which implies a conservative prediction), due to the increased wall roughness the horizontal component drops and the vertical rises, which makes the specific Rankine solution less conservative than the general stress solution. *Second*, for L-shaped cantilever walls, the Rankine solution would be suitable, without any loss of accuracy or violation of a strength criterion, as shown by Kloukinas & Mylonakis [32]. *Third*, if one attempts to verify the value $\delta_R = 26.7^o$ predicted from Eq. (16), it is evident that Eq. (9) can be satisfied only by the modified value $-\pi + \delta_R$. This means that in some cases, deriving the solution requires considering trigonometric roots of the inverse tangent in the form $\pm n\pi + \delta_R, n = 0, 1, 2\ldots$

Considering active conditions under purely gravitational loading ($a_h = a_v = 0$).

- The general stress solution by Mylonakis et al. [35] predicts and active pressure coefficient $K_a = 0.422$, which can be decomposed into a horizontal component $K_{ah} = 0.382$ and a vertical component $K_{av} = 0.178$.
- On the other hand, the Rankine solution yields $\delta_R = 21.8^o$ (Eq. (16)) and $K_a = 0.423$ (Eq. (13)); the latter value can be decomposed into a horizontal component $K_{ah} = 0.377$ and a vertical $K_{av} = 0.191$.

The following observations are worthy of note: *First*, in this case the mobilised wall roughness of 21.8° also exceeds the natural wall roughness of 20°, but the violation is minor. *Second*, the Rankine solution is still less conservative relative to the full stress solution.

A.2 Passive limit state

Considering negative horizontal acceleration $a_h = -0.2$ (i.e. pointing towards the backfill) and $a_v = 0$.

- The general stress solution by Mylonakis et al. [35] predicts a passive pressure coefficient $K_p = 6.31$.
- The Rankine solution predicts $\delta_R = +7.85^o$ (Eq. (16)) and $K_p = 2.97$ (Eq. (13)).

The following observations are worthy of note: *First*, the critical wall roughness of 7.85° is positive and smaller than the actual value of 20°. This suggests that it does not violate the failure criterion at the interface, but it is not physically realizable as it violates the kinematics of the problem which requires a negative roughness. *Second*, the Rankine solution is significantly more conservative relative to the full stress solution.

Considering passive conditions under purely gravitational loading ($a_h = a_v = 0$).

- The general stress solution by Mylonakis et al. [35] predicts a passive pressure coefficient $K_p = 6.55$.
- The Rankine solution yields $\delta_R = +11.87^o$ (Eq. (16)) and $K_p = 2.65$ (Eq. (13)).

The observations for the case with earthquake loading still hold (notably the violation of the problem kinematics), but overall the solution did not change appreciably relative to the seismic case, since passive pressures are less sensitive to seismic excitation.

A.3 Alternative configuration for purely gravitational loading

Considering a problem similar to the previous one, but with horizontal backfill $\beta = 0^o$ and the rest of parameters remaining the same, suffices to demonstrate the importance of different values of wall roughness δ_R.

For an active limit state:

- The general stress solution by Mylonakis et al. [35] predicts an active pressure coefficient $K_a = 0.337$, which can be decomposed int a horizontal component $K_{ah} = 0.305$ and a vertical component $K_{av} = 0.142$.
- The Rankine solution yields $\delta_R = 9.71^o$ (Eq. (16)) and $K_a = 0.345$ (Eq. (13)), which can be decomposed into $K_{ah} = 0.333$ and $K_{av} = 0.09$.

The following observations are worthy of note: *First*, the mobilised wall roughness of 9.71° is positive and smaller than the physical value of 20°, which suggests that the Rankine solution does not violate the kinematics of the problem. *Second*, the Rankine solution is clearly conservative in this case, as it predicts higher pressures overall, plus higher horizontal and lower vertical components.

For a passive limit state.

- The general stress solution by Mylonakis et al. [35] predicts a passive pressure coefficient $K_p = 4.47$.
- The Rankine solution yields $\delta_R = -3.33^o$ (Eq. (16)) and $K_p = 3.00$ (Eq. (13)).

The following observations are worthy of note: *First*, the mobilised wall roughness of -3.33° is negative and smaller, in absolute terms, than the physical value of 20°, which suggests that the Rankine solution, again, does not violate the kinematics of the problem. *Second*, the Rankine solution is still conservative, but its predictions are closer to those of the general stress solution, because the Rankine condition is physically realizable.

Appendix B. Derivation of Equations (16) to (18)

B.1 Derivation of Eq. (16) – Critical wall roughness

- From the active stress tensor shown in Fig. 5:

$$tan\,\delta_R = \frac{\tau_w}{\sigma_w} = \frac{R\,sin(\Delta_2 - \delta_w)}{S - R\,cos(\Delta_2 - \delta_w)} = \frac{sin\,\varphi\,sin(\Delta_{1e} - \beta + \psi_e + 2\omega)}{1 - sin\,\varphi\,cos(\Delta_{1e} - \beta + \psi_e + 2\omega)} \tag{B-1}$$

- Alternative derivation, from Eq. (9):

$$\Delta_2 = \delta_w + \Delta_{1e} - \beta + \psi_e + 2\omega \tag{B-2}$$

$$\frac{sin\,\delta_w}{sin\,\varphi} = sin\left(\delta_w + \underbrace{\Delta_{1e} - \beta + \psi_e + 2\omega}_{\theta}\right) = cos\,\delta_w\,sin\,\theta + sin\,\delta_w\,cos\,\theta \tag{B-3}$$

$$tan\,\delta_w = sin\,\varphi\,sin\,\theta + tan\,\delta_w\,sin\,\varphi\,cos\,\theta = \frac{sin\,\varphi\,sin\,\theta}{1 - sin\,\varphi\,cos\,\theta} \tag{B-4}$$

B.2 Derivation of Eqs. (17) and (18) – Critical slope inclination & critical seismic angle:

- From the stress tensor in Fig. 3a, shown in the Figure below

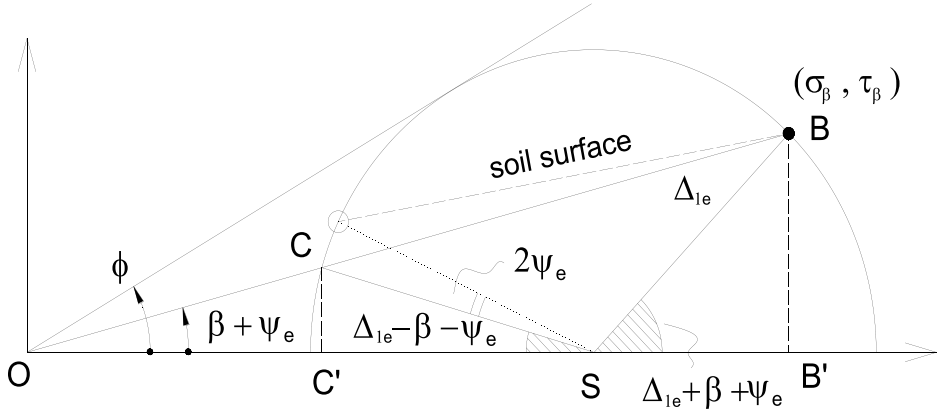

Fig. B1. Stress tensor near the backfill surface (Zona A) for active conditions.

$$tan(\beta_R + \psi_e) = \frac{CC'}{OC'} = \frac{R\,sin(\Delta_{1e} - \beta - \psi_e)}{S - R\,cos(\Delta_{1e} - \beta - \psi_e)} =$$

$$= \frac{sin\,\varphi\,sin(\Delta_2 - \delta_w - 2\omega - 2\psi_e)}{1 - sin\,\varphi\,cos(\Delta_2 - \delta_w - 2\omega - 2\psi_e)} \tag{B-5}$$

and

$$tan(\beta + \psi_{eR}) = \frac{BB'}{OB'} = \frac{R\,sin(\Delta_{1e} + \beta + \psi_e)}{S + R\,cos(\Delta_{1e} + \beta + \psi_e)} =$$

$$= \frac{sin\,\varphi\,sin(\Delta_2 - \delta_w - 2\omega + 2\beta)}{1 + sin\,\varphi\,cos(\Delta_2 - \delta_w - 2\omega + 2\beta)} \tag{B-6}$$

- Alternative derivation, from Eq. (9):

$$\Delta_{1e} = \beta + \Delta_2 - \delta_w - 2\omega - \psi_e \tag{B-7}$$

$$\frac{sin(\beta+\psi_e)}{sin\,\varphi} = sin\left(\beta + \psi_e + \underbrace{\Delta_2 - \delta_w - 2\omega - 2\psi_e}_{\theta}\right) \rightarrow$$

$$tan(\beta+\psi_e) = \frac{sin\,\varphi\,sin\,\theta}{1 - sin\,\varphi\,cos\,\theta} \tag{B-8}$$

or

$$\frac{sin(\beta+\psi_e)}{sin\,\varphi} = sin\left(-(\beta+\psi_e) + \underbrace{\Delta_2 - \delta_w - 2\omega + 2\beta}_{\theta}\right) \rightarrow$$

$$tan(\beta+\psi_e) = \frac{sin\,\varphi\,sin\,\theta}{1 + sin\,\varphi\,cos\,\theta} \tag{B-9}$$

B.3 Derivation of Eq. (19) – Critical soil friction angle

- From Eq. (9):

$$\Delta_2 - \Delta_{1e} = \underbrace{\delta_w - \beta + \psi_e + 2\omega}_{\theta} \tag{B-10}$$

Using the trigonometric identity:

$$sin^{-1}\,a - sin^{-1}\,b = sin^{-1}\left(b\sqrt{1-a^2} - a\sqrt{1-b^2}\right) \tag{B-11}$$

we get

$$\frac{sin\,\delta_w}{sin\,\varphi}\sqrt{1-\left[\frac{sin(\beta+\psi_e)}{sin\,\varphi}\right]^2} - \frac{sin(\beta+\psi_e)}{sin\,\varphi}\sqrt{1-\left[\frac{sin\,\delta_w}{sin\,\varphi}\right]^2} = sin(\theta) \tag{B-12}$$

Solving the equation with respect to sinφ, we obtain

$$sin\,\varphi = \frac{1}{sin\,\theta}\sqrt{sin^2\delta_w + sin^2(\beta+\psi_e) - 2\,sin\,\delta_w\,sin(\beta+\psi_e)cos\,\theta} \tag{B-13}$$

References

[1] Rankine WJM. On the stability of loose earth. Phil Trans Roy Soc Lond 1857;147:9–27.
[2] Nadai A. Theory of flow and fracture of solids. New York: McGraw-Hill; 1963.
[3] Sokolovskii VV. Statics of granular media. New York: Pergamon Press; 1965.
[4] Heyman J. Coulomb's Memoir on Statics; an essay in the history of civil engineering. Cambridge University Press; 1973.
[5] Chen WF. Limit analysis and soil plasticity. Developments in geotechnical engineering. Amsterdam: Elsevier; 1975.
[6] Atkinson J. Foundations and slopes. London: McGraw Hill; 1981.
[7] Davis RO, Selvadurai APS. Plasticity and geomechanics. Cambridge: Cambridge University Press; 2002.
[8] Powrie W. Soil mechanics: concepts & applications. third ed. London: CRC Press; 2018.
[9] Müller - Breslau H. Erddruck auf stützmauern, Kroener. Stuttgart: Germany; 1906 [in German].
[10] Barré de Saint-Venant AJC. Sur l'établissement des équations des mouvements intérieurs opérés dans les corps solides ductiles au-delà des limites où l'élasticité pourrait les ramener à leur premier état. C R Acad Sci Paris 1870;70:473–80 [Reprinted (1871) J Math Pures Appl 16:308–316].
[11] Lévy M. Sur une théorie rationnelle de l'equilibre des terres fraîchement remuées et ses applications au calcul de la stabilité des murs de soutènement. 357 Journal de Mathématiques, 2nd series 1873;18:241.
[12] Boussinesq J. Essai théorique sur l'équilibre d'élasticité des massifs pulvérulents et sur la poussée des terres sans cohésion. Mémoires Savante Étrangère, Académie Royale de Belgique 1876;40:1–80.
[13] Kötter F. Die Bestimmung des Drucks an gekrümmten Gleitflächen eine Aufgabe aus der Lehre vom Erddruck Sitzungsberichte der Akademie der Wissenschaften. 1903. p. 229–33. Berlin.
[14] Karman von T. Uber elastische grenzzustände, proceedings of the second international congress of applied mechanics. Zurich: p.23; 1927.
[15] Abbott BM. An introduction to the method of characteristics. NY: Elsevier; 1967.
[16] Kerisel J, Absi E. Active and passive earth pressure tables. A.A. Balkema; 1990.
[17] Caquot A. *Équilibre des massifs à frottement interne.* Gauthier-Villars. 1934 [Paris].
[18] Chu SC. Rankine analysis of active and passive pressures in dry sands. Soils Found 1991;31(4):115–20.
[19] Greco VR. Stability of retaining walls against overturning. Journal of Geotechnical & Geoenvironmental Engineering, ASCE 1997;123(8):778–80.
[20] Greco VR. Active earth thrust on cantilever walls in general conditions. Soils Found 1999;39(6):65–78.
[21] Budhu M. Soil mechanics & foundations. third ed. 2010 [J. Wiley & Sons Inc, New York].
[22] Fernandes MM. Analysis and design of geotechnical structures, CRC press, taylor and francis group, New York. https://doi.org/10.1201/9780429398452; 2020.
[23] Iskander M, Omidvar M, Elsherif O. Conjugate stress approach for Rankine seismic active earth pressure in cohesionless soils. J Geotech Geoenviron Eng 2013;139(7):1205–10. https://doi.org/10.1061/(ASCE)GT.1943-5606.0000830.
[24] Ebeling RM, Morrison EE, Whitman RV, Liam Finn WD. A manual for seismic design of waterfront retaining structures, US army corps of engineers. Technical Report ITL 1992:92. 11.
[25] Kloukinas P. Contribution to the static and dynamic analysis of retaining walls by means of theoretical and experimental methods. PhD thesis. University of Patras; 2012 [in Greek].
[26] Shamsabadi A, Xu S, Taciroglu E. A generalized log-spiral-Rankine limit equilibrium model for seismic earth pressure analysis. Soil Dynam Earthq Eng 2013;49:197–209.
[27] Xu SY, Shamsabadi A, Taciroglu E. Nonlinear force-displacement relationship of earth retaining structures: an alternative approach based on the log-spiral-hyperbolic method. In: Paper presented at 2014 global civil engineering & applied science conference. Taipei: Taiwan; 2014. p. 90–101.
[28] Giarlelis C, Mylonakis G. Interpretation of retaining wall dynamic model tests in light of elastic and plastic solutions. Soil Dynam Earthq Eng 2011;31(1):16–24.

[29] Kloukinas P, di Santolo AS, Penna A, Dietz M, Evangelista A, Simonelli AL, Taylor C, Mylonakis G. Investigation of seismic response of cantilever retaining walls: limit analysis vs shaking table testing. Soil Dynam Earthq Eng 2015;77:432–45.
[30] Terzaghi K. Theoretical soil mechanics. New York: John Wiley & Sons Inc.; 1943.
[31] Evangelista A, Scotto di Santolo A, Simonelli AL. Evaluation of pseudostatic active earth pressure coefficient of cantilever retaining walls. Soil Dynam Earthq Eng 2010;30(11):1119–28.
[32] Kloukinas P, Mylonakis G. Rankine Solution for seismic earth pressures on L-shaped retaining walls. In: *Proceedings of 5th international Conference on earthquake geotechnical engineering.* Santiago, Chile; 2011.
[33] Lancellotta R. Analytical solution of passive earth pressure. Géotechnique 2002;52(8):617–9.
[34] Lancellotta R. Lower-bound approach for seismic passive earth resistance. Géotechnique 2007;57(3):319–21.
[35] Mylonakis GE, Kloukinas P, Papantonopoulos C. An alternative to the Mononobe–Okabe equations for seismic earth pressures. Soil Dynam Earthq Eng 2007;27(10):957–69.
[36] Caquot A, Kerisel L. *Traité de mécanique des sols.* Gauthier-Villars. 1948 [Paris].
[37] James RG, Bransby PL. Experimental and theoretical investigations of a passive pressure problem. Géotechnique 1970;20(1):17–37.
[38] Sheriff MA, Ishibashi I, Lee CD. Earth pressures against rigid retaining walls. J Geotech Eng, ASCE 1982;108(GT5):679–96.
[39] Fang YS, Ishibashi I. Static earth pressures with various wall movements. Journal of geotechnical engineering. ASCE 1986;112(3):317–33.
[40] Potts DM, Fourier AB. A numerical study of the effects of wall deformation on earth pressures. Int J Numer Anal Methods GeoMech 1986;10:383–405.
[41] Shiau JS, Augarde CE, Lyamin AV, Sloan SW. Finite element analysis of passive earth resistance in cohensionless soils. Soils Found 2008;48(6):843–50.
[42] James RG, Bransby PL. A velocity field for some passive earth pressure problems. Géotechnique 1971;21(1):61–83.
[43] Fang YS, Chen TJ, Wu BF. Passive earth pressures with various wall movements. Journal of geotechnical engineering. ASCE 1994;120(8):1307–23.
[44] Bolton MD, Powrie W. Behaviour of diaphragm walls in clay prior to collapse. Géotechnique 1988;38(2):167–89.
[45] Nakamura S. Re-Examination of mononobe–okabe theory of gravity retaining walls using centrifuge model tests. The Japanese Geotechnical Society, Soils and Foundations 2006;46(2):135–46.
[46] Papantonopoulos C, Ladanyi B. Analyse de la Stabilité des Talus Rocheux par une Méthode Généralisée de l'Equilibre Limite. In: proceedings, ninth Canadian rock mechanics symposium. Montreal December 1973:167–96 [in French].
[47] Costet J, Sanglerat G. Cours pratique de mécanique des sols, plasticité et calcul des tassements. second ed. Paris: Dunod Technique Press; 1975.
[48] Soubra AH. Static and seismic passive earth pressure. Can Geotech J 2000;37:463–78.
[49] Considère A. Sur la Poussée des Terres, Annales des Pont et Chaussées. 4th Series 1870;256:547–94.
[50] Fang YS, Chen JM, Chen CY. Earth pressures with sloping backfill. Journal of Geotechnical & Geoenvironmental. Engineering, ASCE 1997;123(3):250–9.
[51] Clayton CRI, Militisky J, Woods RI. Earth pressure and earth retaining structures. second ed. 1993 [Blackie Acad.. & Prof].
[52] Trenter NA. Approaches to the design of cantilever retaining walls. Proc Inst Civ Eng: Geotech Eng 2004;157(1):27–35.
[53] O'Sullivan C, Creed M. Using a virtual back in retaining wall design. Proc Inst Civ Eng: Geotech Eng 2007;160(GE3):147–51.
[54] Brandenberg SJ, Mylonakis GE, Stewart JP. Kinematic framework for evaluating seismic earth pressures on retaining walls. J Geotech Geoenviron Eng 2015;141(7):04015031.
[55] Brandenberg SJ, Mylonakis GE, Stewart JP. Approximate solution for seismic earth pressures on rigid walls retaining inhomogeneous elastic soil. Soil Dynam Earthq Eng 2017;97:468–77.
[56] Brandenberg SJ, Durante MG, Mylonakis GE, Stewart JPS. Winkler solution for seismic earth pressures exerted on flexible walls by vertically inhomogeneous soil. J Geotech Geoenviron Eng 2020;146(11):04020127.
[57] Durante MG, Stewart JP, Brandenberg SJ, Mylonakis G. Simplified solution for seismic earth pressures exerted on flexible walls. Earthq Spectra 2022;38(3):1872–92.
[58] Conti R, Caputo VG. A numerical and theoretical study on the seismic behaviour of yielding cantilever walls. Géotechnique 2018;69(5):1–47. 10.1680/jgeot.17.p.033.
[59] Coulomb CA. Essai sur une application des règles de maximis et minimis à quelques problèmes de statique relatifs à l'architecture. Mémoires de Mathématique et de Physique. Présentés a l' Académie Royale des Sciences; Paris 1776;7:343–82.

List of Main Symbols

A: width of soil element
a_h, a_v: horizontal and vertical pseudo-static seismic acceleration
f_h, f_v: horizontal and vertical body forces in the soil element
f_q: vertical force on the soil element due to surcharge
$K_{\gamma E}$, K_{qE}: seismic earth pressure coefficients due to self-weight & surcharge
N, T: reactions at the base of the soil element
P_E: overall seismic thrust on the wall
q: surcharge on backfill surface
S_A: mean stress (centre of Mohr circle)
β, β_R: backfill inclination; critical value to satisfy Rankine condition
γ: soil unit weight
δ_w, δ_R: wall roughness; critical value to satisfy Rankine condition
$\delta_{m\theta}$: traction inclination ("mobilised fiction") on arbitrary plane in the soil
Δ_{1e}, Δ_2: auxiliary Caquot angles
$\theta_{1B,\alpha}$: inclination of major principal plane from the horizontal
θ_{AB}: angle separating zones A and B
σ_β, τ_β: normal and shear stresses acting parallel to soil surface
σ_θ, τ_θ: normal and shear stresses acting parallel to an arbitrary plane
σ_w, τ_w: normal and shear component of soil-wall contact traction
φ, φ_R: friction angle; critical value to satisfy Rankine condition
ψ_e, ψ_{eR}: inclination of combined gravitational/earthquake body force; critical value to satisfy Rankine condition
ω, ω_R: wall inclination; critical value to satisfy the Rankine condition